Experimental investigation of a five WECs array hydrodynamics

Sergej Antonello Sirigu[#1], Mauro Bonfanti[#2], Panagiotis Dafnakis[#3], Giovanni Bracco[#3], Giuliana Mattiazzo[#3]

[#]*Department of Mechanichal and Aerospace Engineering (DIMEAS), Polytechnic of Turin*
Corso Duca d'Abruzzi 24, Turin, Italy

[1]Sergej.Sirigu@polito.it

[2]Mauro.Bonfanti@polito.it

[3]Panagiotis.Dafnakis@polito.it

[4]Giovanni.Bracco@polito.it

[5]Giuliana.Mattiazzo@polito.it

***Abstract*—In this paper, the experimental test of five 1:20 scale pitching floating Wave Energy Converters (WEC) arranged in two different array layouts is presented and described. A particular attention is given to the challenging experimental setup and the first analysis of the hydrodynamic interaction occurring among the different bodies. The Response Amplitude Operators (RAO) of the array WECs are compared against the dynamics of the isolated floater test, in order to evaluate the bodies' interaction and thus the devices performances. The regular waves are performed for two wave steepness 1:50 and 1:35. A free decay analysis is conducted in order to identify the natural frequency, linear and quadratic damping term for the pitch Degree of Freedom (DoF).**

***Keywords*— Wave Energy Converter, Array, Hydrodynamics, Experimental, Tests, ISWEC, Scaled Model, Wave Basin**

I. INTRODUCTION

Nowadays floating WECs represent a large segment of the technological solution in the wave energy-harvesting field [1]. Several devices reached the phase of full scale prototypes and have been tested in open sea [2].

At this stage the economical, reliability and feasibility of the technology is fundamental. It has long been established the advantage of harvesting the wave energy via array of devices instead of the deployment of a single device with high power capacity [3]. Therefore, with the aim of maximize the extraction of energy via optimization of the number of devices and their relative position has been analysed by different authors [4-6]. These analytics and numerical methods present some limits due to the restrictive assumption adopted to facilitate the analysis and further information can be found in [7]. Unfortunately, the hydrodynamic interaction between the floaters is complex and not trivial to model. In the case of floaters that are not constrained in a fixed position the assumption of constant hydrodynamic coupling coefficients cannot be considered valid. Moreover, additional complexity can derive from the presence of the mooring systems, and it has been demonstrated that a quasi-static approach is not enough to describe its dynamics and dynamic models are necessary [8, 9].

Therefore, CFD and experimental tests can be carried out in order to analyse the dynamics of the floaters in an array including all the complex interactions. In [10] the author demonstrate the agreement between CFD and experimental results for a single wave energy converter and then the feasibility of this numerical approach. The CFD studies on the interaction between floaters in an array has been so far poorly investigated. In [11] the authors present an introduction of the CFD modelling of two WECs without the presence of the mooring system. In [12] a CFD modelling of an entire array of floating WECs is presented, but due to the technology solution there is not the presence of the mooring system and the motion of the single floaters is constrained and only a vertical motion is allowed. Experimental campaign tests on scaled model are the most representative of the real scaled model dynamics and different investigations have been carried out by different authors [13-16].

In this paper, the authors present the experimental test campaign on an array of five floating scaled WECs in order to investigate the hydrodynamic behaviour of the array. The tests has been carried out in February 2018 in the LHEEA Hydrodynamic and Ocean Engineering Tank at the Ecole Centrale in Nantes. The devices that have been tested are a 1:20 scaled models of the ISWEC (Inertial Sea Wave Energy Converter) prototype developed in Polytechnic of Turin and the full-scale prototype has been tested successfully in the period October-December 2015. The description and working principle are described exhaustively in [17-18]. Each device present a slack mooring system that allows the device to align itself with the incoming sea state. The ISWEC is a pitching floating device that harvest the wave energy through a gyroscopic system enclosed in a watertight hull. The PTO converts the mechanical energy of the precession motion of the gyroscope in electrical power. Analysing the dynamic equation presented in [19] is possible to conclude that the extracted energy is function only of the pitch motion of the floater. Therefore, the pitch Response Amplitude Operator can be adopted as an index of the performances of the single devices in an array. In this preliminary work, only the floaters dynamics is considered, the gyroscopic system is not included

in this experimental investigation in order to underline and study only the hydrodynamic behaviour of interacting floating bodies.

II. Experimental Setup

A. WEC Model

In this experimental campaign, five identical models were adopted. The floaters are 1:20 scaled prototypes of the ISWEC device designed for the Pantelleria Island site [17]. The Froude scaling law have been used to scale down the geometrical and inertial properties of the model. Fig. 1 shows the CAD model highlighting all the functional parts and the scaled down properties derived from CAD are listed in TABLE 1.

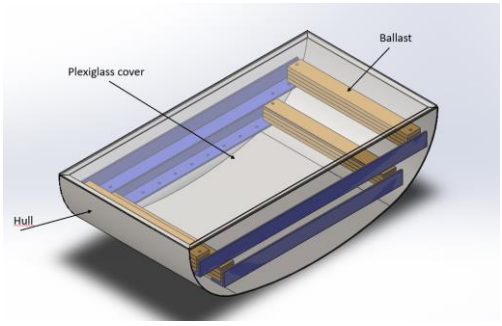

Fig. 1 CAD model of the 1:20 tested prototype

TABLE 1
Geometrical and inertial properties of the tested model from CAD

Variable	Unit	Value
Length	mm	766
Heigth	mm	225
Width	mm	400
Mass	kg	33.2
Inertia I_{xx}	kgm^2	0.73
Inertia I_{yy}	kgm^2	2.33
Inertia I_{zz}	kgm^2	2.87
Draft	mm	150
COG from deck	mm	102

Fig. 2 shows the five models ready for the experimental tests. Every model was weigthed before and after the assembly of the motion capture system markers and in TABLE 2 the measured mass values are shown.

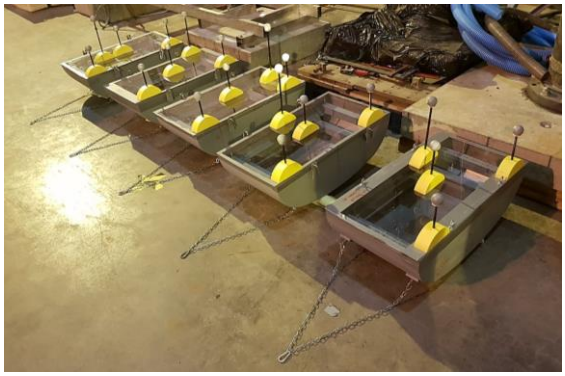

Fig. 2 Five 1:20 models ready for the experimental tests

TABLE 2
Measured mass of each 1:20 model

Variable	Unit	Model 1	Model 2	Model 3	Model 4	Model 5
Floater mass	kg	34.3	34.6	34.7	34.6	35.0
Total mass with markers	kg	34.5	34.8	34.9	34.8	35.2

The draft and static stability of each model was checked before the experimental tests in the shallow water tank of the LHEEA facility.

B. Mooring system

Fig. 3 shows the mooring system configuration adopted in this experimental campaign. The mooring system consists essentially in 1 bottom chain line L_1 anchored to the artificial sea bed and connected to the jumper. Two chain bridles L_3 connect the device to a mechanical joint and another chain line L_2 connect it to the jumper. The mooring system is designed to allow the weathervaning of the device, to influence as little as possible the pitch motion and to present a satisfying behaviour in extreme weather conditions.

Gravity and inertia forces principally govern the dynamic behaviour of this system. Therefore, the mooring system was scaled as done for the floater model with the Froude scaling law and a scaling factor $\lambda = 20$.

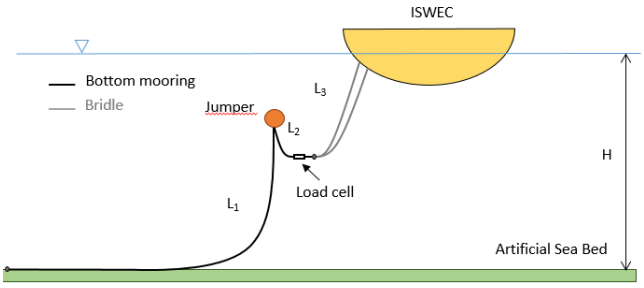

Fig. 3 Single device mooring configuration

TABLE 3 lists the scaled down properties of the mooring system. The net buoyancy of the jumpers was checked experimentally with calibrated masses to guarantee a net buoyancy of 190 g.

TABLE 3
MOORING SYSTEM PROPERTIES

Variable	Unit	Value
Geometry		
Artificial sea bed, H	m	1.25
Anchor-Jumper length, L1	m	3.25
Jumper-Bridle length, L2	m	0.5
Bridle-ISWEC length, L3	m	0.5
Chain Properties for Bottom Lines		
Nominal Diameter, D1	mm	3
Mass per unit length (Datasheet)	kg/m	0.186
Mass per unit length (Measured)	kg/m	0.149
Chain Properties for Bridle Lines		
Nominal Diameter, D2	mm	2.2
Mass per unit length (Datasheet)	kg/m	0.09
Mass per unit length (Measured)	kg/m	0.08
Jumper Properties		
Net Buoyancy, B	g	190

A Genovese type chain was adopted for all the mooring lines, the wire diameter and mass per unit length were directly scaled from full-scale.

Fig. 4 shows the complete mooring system configuration during a test with all the connection components. The bottom line chain was anchored directly to the steel tube of the artificial seabed, not shown in figure. The mooring system of each device was provided with a load cell mounted as shown in Fig. 3 and Fig. 4. The linear characteristics was tested until 10 kg at 6 V, and the saturation was at 10 V, and therefore the maximum measurable value was about 16 kg.

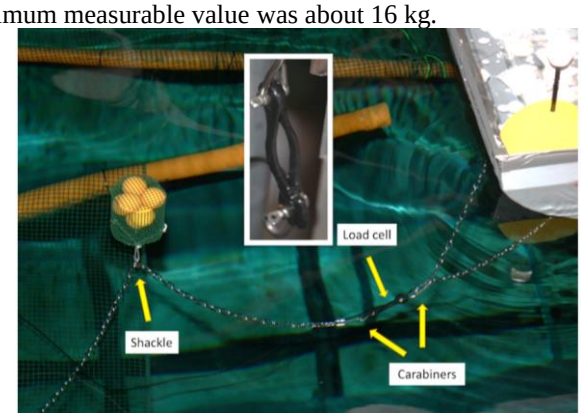

Fig. 4 Mooring system configuration during test

C. Wave Tank

The test campaign has been carried out in February 2018 at the hydrodynamic and ocean engineering tank of the LHEEA Centrale Nantes inside the MARINET2 project. The tank is 50 m long, 30 m wide and 5 m deep. The basin is equipped with a segmented wave maker, composed of 48 hinged flaps distributed over the width of the basin. Each flap is controlled in position separately. The wave generator system is equipped with an active wave absorption (force) control feature.

The other end of the basin is composed of a 7m passive wave breaking beach (gentle slope and quadratic profile).

The wavemaker control software gives access to the following high quality waves :

- Regular and irregular waves
- Unidirectional / directional waves
- Irregular crossing waves (angle up to 90°)

Wave parameter range:

- Periods T 0.5 to 5.0 s
- Regular wave height H max 1.0 m
- Irregular wave height Hs max 0.8 m

Fig. 5 Picture of the facility during a test

D. Artificial Sea Bed

To ensure the seabed distance in the scaled configuration and therefore the validity of the results, five artificial seabeds have been used for each model to recreate the depth of the site where the full-scale prototype will be deployed. The artificial seabeds were made using Ø48 mm steel bars and PVC pipes connected by orthogonal joints in order to create the structure shown in Figure 2.14. The seabed was built using a plastic grid stretched to ensure as much as possible its flatness.

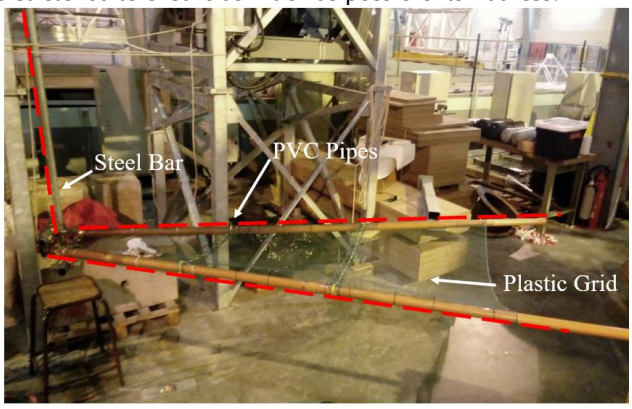

Fig. 6 Artificial seabed structure

Every artificial seabed were mounted on the wave basin footbridge as shown in Fig. 7 through the use of five steel bar interfaces. Orthogonal joints allowed also an easy calibration of the right vertical positioning of each artificial seabed.

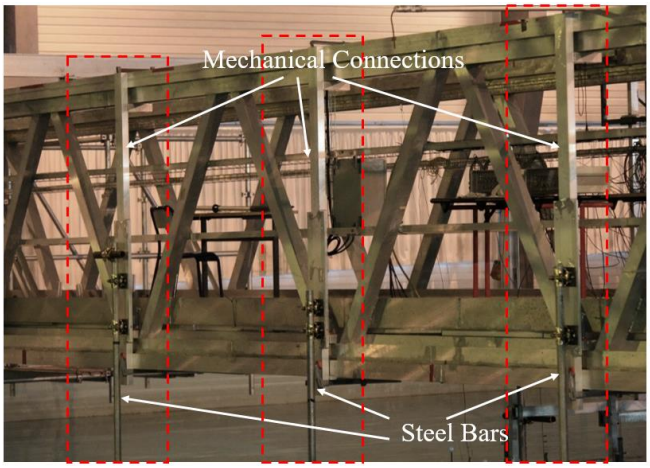

Fig. 7 Mechanical connection interface between the wave tank footbridge and the artificial seabeds

Fig. 8 shows the five seabeds layout and the main distances. The mooring lines of each devices were laid down on the artificial seabed and they were anchored on each steel bar.

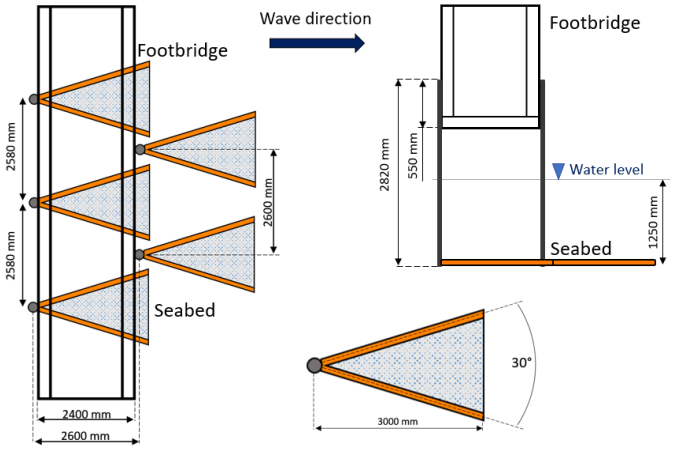

Fig. 8 Artificial Seabed layout and main distances

E. *Motion Capture System*

In order to capture the bodies' motions the optical motion tracking system Qualisys of the LHEEA facility were used. Each body presents one marker exactly above the COG of the floater, and other two markers are installed in order to identify a plane X-Y of the body. Qualisys light markers with a diameter of 40 mm were used and fixed on a polystyrene support through carbon sticks. Afterwards the marker supports were attached on the floater decks through double-sided adhesive tape as shown in Fig. 2. A fourth marker was attached in each deck floater in a random position in order to let the Qualisys system distinguish properly each body.

The parallelism of each floater deck were checked with a bubble level. Afterwards, a 360 degree self-levelling line laser was used in order to set up the three markers that identify the plane X-Y.

Five cameras were used to acquire the motion of each body and the whole motion capture system was properly calibrated before the beginning of the experimental test campaign.

F. *Wave Probes*

In order to measure the undisturbed and disturbed wave field an array of 15 resistive wave probes were provided by the LHEEA facility and installed following the layout sketched in Fig. 9.

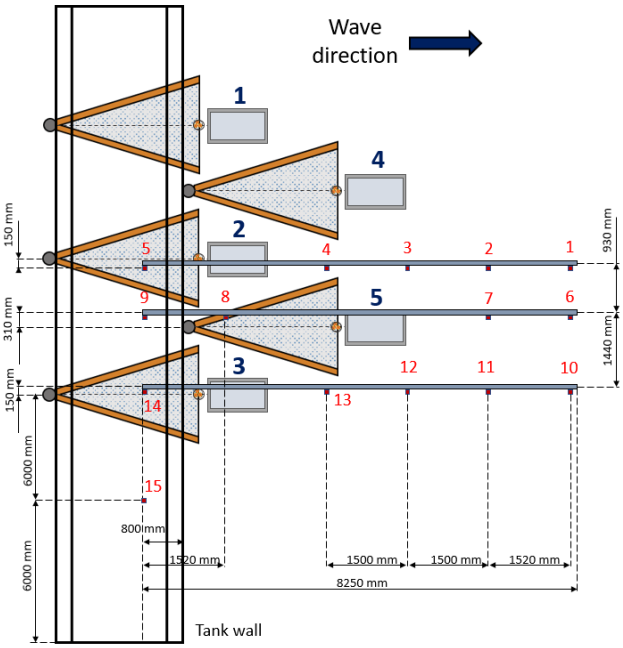

Fig. 9 Plan view of the wave probes layout and disposition of the five artificial seabeds and floaters

Each model has a working area of maximum 4.7 m from the anchoring point corresponding to the maximum elongation of the mooring lines. This distance was taken into account during the wave probes layout study, in order to avoid any collision between devices and wave probes. Three triangular aluminium bars were mounted on the main footbridge in order to allow the installation of the wave probes as shown in Fig. 10.

Fig. 10 Wave probes mounting solution

G. *Data Acquisition System*

A National Instrument data system (NI-PCI-6225) was used during the tests to acquire all the signal channels coming from the 5 load cells and the 15 wave probes, which were appropriately conditioned and amplified.

Fig. 11 shows the signal routing and data acquisition architecture. A 5V TTL trigger signal was used to synchronize the analogical signals were acquired by the NI acquisition system and all the signals are sampled with 100 Hz frequency. The final output data is a txt file with all the wave probes signals, load cells, and DoFs of each device. The data elaboration is made with Matlab.

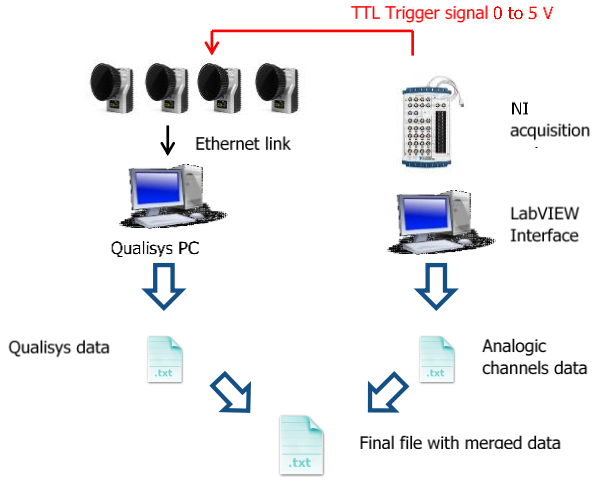

Fig. 11 Data acquisition system

III. Results

This section describes the results obtained by the experimental campaign, showing the critical aspects of the analysis of the results as well as the results themselves.

A. *Free Decay Analysis*

Free decay tests were conducted for pitch degree of freedom considering only the floater without the mooring. The free decay analysis has the objective to identify the natural period of the single device and to extrapolate the linear and quadratic damping term. During the free decay tests, the water in the wave tank was as much still as possible and a member of the team positioned the floater with a pitch offset and then released in order to have free oscillation. The Camera acquisition system measured every free decay and in Fig. 12 the rough signals obtained from the tests are shown.

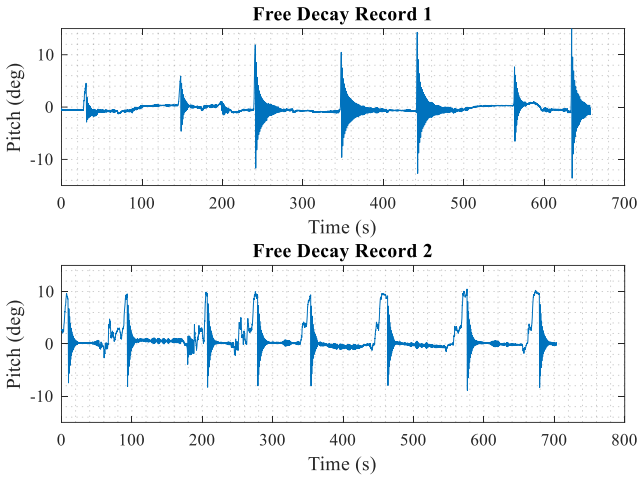

Fig. 12 Rough free decay signals

All the data taken from the experiments were elaborated in Matlab environment. Every free decay record was cut in order to eliminate the first oscillation and considering a minimum oscillation of 1 deg and an operation of signal cleaning and filtering was carried out. A low pass Butterworth filter with order 4 was used with a cutting frequency of 4 Hz, 4 times the natural period of the pitch DoF. In order to carry out an adequate free decay analysis the elimination of mean values and linear trends from the decay record is necessary and the filtering result is shown in Fig. 13.

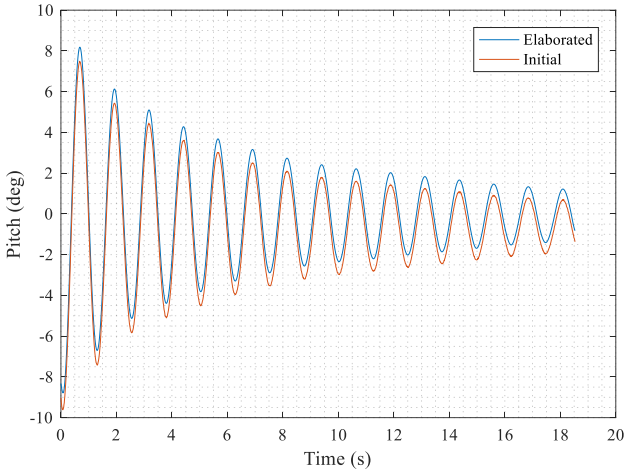

Fig. 13 Rough and filtered signal comparison

For the identification of the linear and the non-linear quadratic damping, the identification method presented in [20] was used. The equations presented in the paper were used in order to identify the damping coefficients for the roll motion of naval ships and with reference to the work of Chakrabati [21], Bulian et al [22] and the ITTC Recommended

Procedures and Guidelines. Numerical Estimation of Roll Damping [23]. However, they can be applied without any problem in the identification of the damping coefficient for the pitch motion of 1:20 ISWEC model. It was assumed that dynamics can be described by a single degree of freedom. Using the same nomenclature of the reference paper the pitch dynamics during a free decay test can be modelled and expressed as:

$$\ddot{\varphi} + 2\alpha\dot{\varphi} + \beta\dot{\varphi}|\dot{\varphi}| + \omega_n^2\varphi = 0$$

Where

- Φ is the pitch DoF variable
- α is the linear damping coefficient
- β is the quadratic damping coefficient
- ω_n is the natural frequency in rad/s

The objective of the free decay analysis is the identification via logarithmic decrease method of the damped natural frequency, linear and quadratic damping of the model in analysis. The calculated equivalent roll extinction coefficient for the pitch DoF as a function of the pitch mean amplitude is given in Fig. 14 with the linear regression curve. The intercept on the y-axis represents the linear damping component and the angular coefficient of the regression curve represents the quadratic damping term.

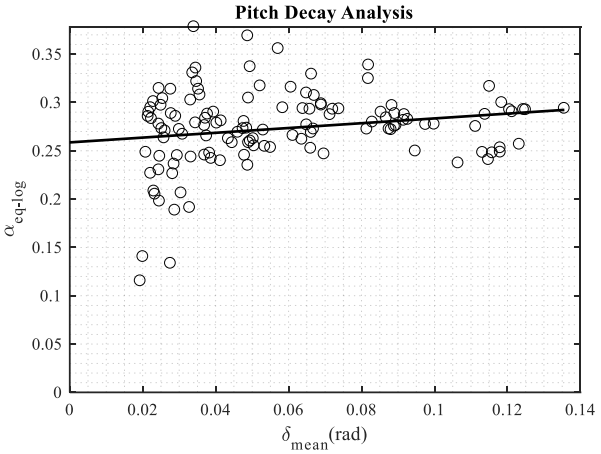

Fig. 14 Linear regression curve αeq-log

The results of the pitch decay experiments are given in TABLE 4.

TABLE 4
Free Decay Analysis Results

Variable	Unit	value
Damped natural period, T	s	1.060
Angular coefficient of the regression curve, a	1/s	0.248
y-axis intercept of the regression curve, b	1/s	0.259
Linear extinction coefficient, α	1/s	0.259
Quadratic extinction coefficient, β	1/rad	0.099

B. *Regular Wave Analysis*

A regular wave analysis was carried out in order to identify the dimensionless pitch RAO (Response Amplitude Operator) of the floaters defined as:

$$\mathrm{RAO}_{55} = \frac{\eta_5}{\mathrm{ka}}$$

Where η_5 is the pitch DoF, *k* is the wave number and *a* is the wave amplitude. Waves with direction 0° and two different steepness 1/50 and 1/35 were generated and tested for two different array configurations and the results are compared with the RAO of the single device configuration. The wave test list is shown in and Table 10. With reference to Fig. 8, the array configurations that have been studied are the 3x1 array layout, composed by the models number *1, 2, 3* and the 3x2 array layout composed by the models number *1, 2, 3, 4, and 5*.

TABLE 5
Regular Waves Test Plan

Wave n°	Freq (Hz)	T (s)	H (mm)	a (mm)
Steepness 1/50				
wave 1	1.2	0.833	21.7	10.8
wave 2	1118	0.894	25	12.5
wave 3	1052	0.951	28.2	14.1
wave 4	0.994	1006	31.6	15.8
wave 5	0.952	1.050	34.5	17.2
wave 6	0.894	1119	39.1	19.5
wave 7	0.8131	1230	47.2	23.6
wave 8	0.745	1342	56.3	28.1
wave 9	0.639	1565	76.5	38.2
wave 10	0.559	1.789	99.9	50
Steepness 1/35				
wave 11	1118	0.89	35.7	17.8
wave 12	1052	0.95	40.3	20.2
wave 13	0.994	1.01	45.1	22.6
wave 14	0.952	1	49.2	24.6
wave 15	0.894	1.12	55.8	27.9
wave 16	0.813	1.23	67.5	33.7
wave 17	0.745	1.34	80.4	40.2
wave 18	0.639	1.56	109.2	54.6

Purpose of these experimental tests is a first investigation on the hydrodynamic behaviour and performances of two array configurations in regular wave.

Data processing involved both the DoF signals coming from the capture motion system and from the resistive wave probe. In order to calculate the wave amplitude of the

undisturbed wave field, the wave probe number 15 has been chosen for this purpose.

Signals of each test are manually processed in Matlab environment. The signals are properly cut in such a way to choose a time interval of analysis where the floaters dynamics reach a stationary condition. The data is subsequently filtered with a Butterworth low-pass filter with a frequency cut-off of 10 Hz, ten times the characteristic frequency of the physical phenomenon in order to eliminate the measurement chain noise. An FFT analysis is then carried out to obtain the signal frequency and amplitude of each floater DoF measured by QualiSys system and wave probe measurement.

The stationary condition was not difficult to reach for the case of single device configuration, 3x1 array configuration and for the case of long period wave tests where the diffraction and radiation wave fields are not predominant. Fig. 15 shows the pitch motion of each floater for the wave test 10 3x2 array configuration and as said before for long waves the stationarity condition is reached. Instead, Fig. 16 shows the pitch motion for the wave test 5 3x2 array configuration, that present a wave period close to the pitch natural period of the device. In this case, the pitch motion does not show any stationary condition for any floater. Close to the resonance condition, the diffraction and radiation wave fields become relevant in comparison to the incident wave field and therefore the motion of one floater affects the motion of the other floaters and no stationary condition can be reach for a regular wave analysis.

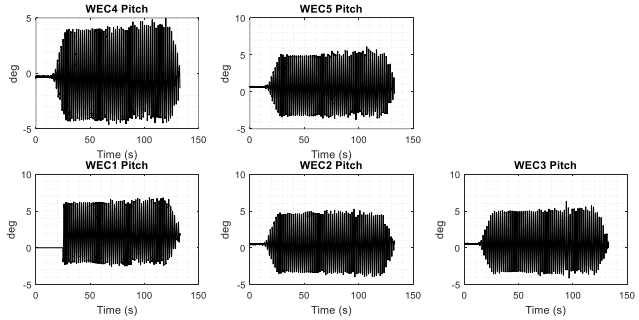

Fig. 15 Regular wave test – Steepness 1:50 – Freq = 0.559 Hz, H = 99.9 mm – 3x2 Array configuration – Pitch motion

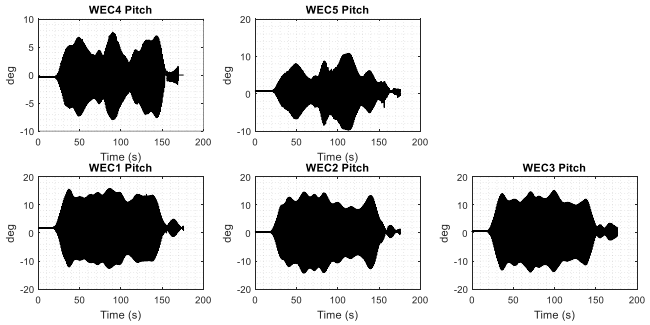

Fig. 16 Regular wave test – Steepness 1:50 – Freq = 0.952 Hz, H = 34.5 mm – 3x2 Array configuration – Pitch motion

For the sake of completeness, the surge, sway and yaw motion of the floaters for the wave case test 10 and 5 are given.

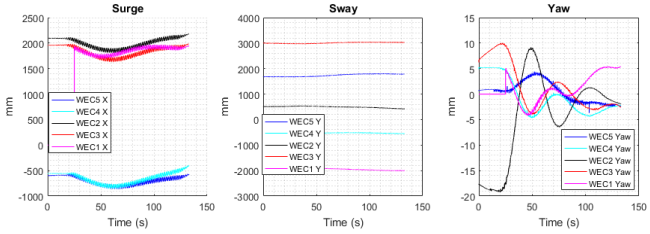

Fig. 17 Regular wave test – Steepness 1:50 – Freq = 0.559 Hz, H = 99.9 mm – 3x2 Array configuration

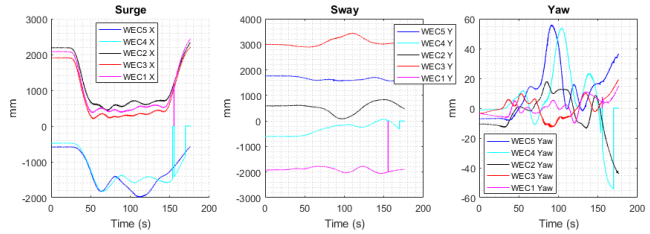

Fig. 18 Regular wave test – Steepness 1:50 – Freq = 0.952 Hz, H = 34.5 mm – 3x2 Array configuration

Fig. 19 and Fig. 20 show the dimensionless pitch RAO of each device in the array configuration 3x1 compared to the single device configuration for both the wave steepness for both the wave steepness cases.

The maximum of the dimensionless pitch RAO is between 1.05 s and 1.118 s, as expected from the free decay analysis where the natural period is 1.06 s and the hydrodynamic behaviour of the floaters in 3x1 configuration is similar to the single device configuration.

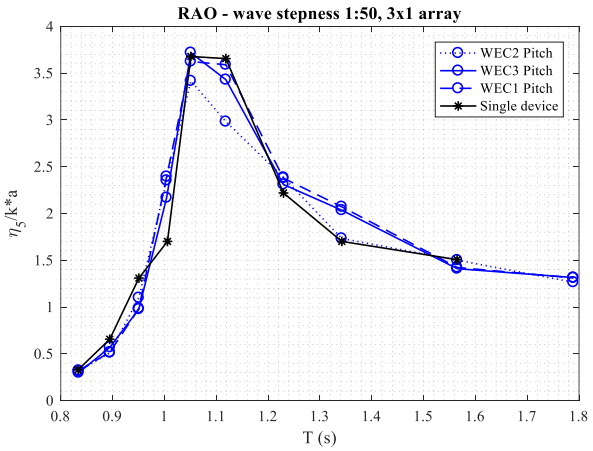

Fig. 19 Dimensionless pitch RAO – Array configuration 3x1 – Wave steepness 1:50

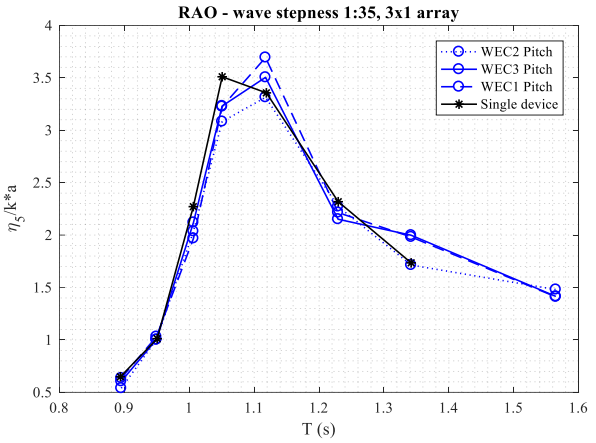

Fig. 20 Dimensionless pitch RAO – Array configuration 3x1 – Wave steepness 1:35

Instead, in Fig. 21 and Fig. 22 the dimensionless pitch RAO of the 5 devices in the array configuration 3x2 in comparison to the single device test case for both wave steepness 1/50 and 1/35. For high frequencies, the quantitative results are less reliable in comparison to the single device test case as said before due to the no realization of stationary conditions.

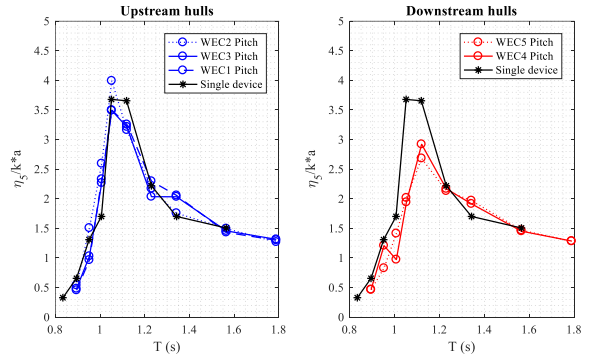

Fig. 21 Dimensionless pitch RAO – Array configuration 3x2 – Wave steepness 1:50

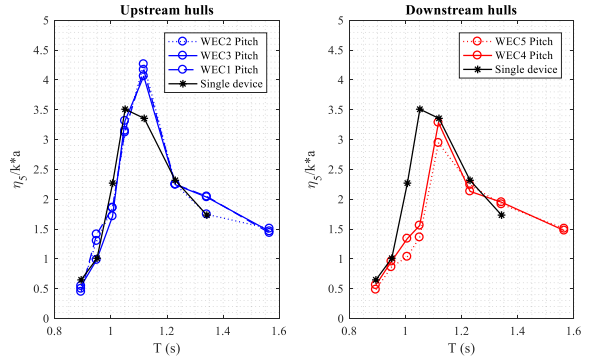

Fig. 22 Dimensionless pitch RAO – Array configuration 3x1 – Wave steepness 1:35

Qualitatively it is possible to say that the interaction between the floaters is relevant close to the pitch natural period. The two floaters *4* and *5* positioned downstream are negatively affected by the presence of the floaters *1, 2, 3* positioned upstream with a decrease of performances. Instead, the three floater positioned upstream present a behaviour similar to the isolated one. This reduction will reflect negatively the performance of the devices and they will present a lower annual productivity in this array configuration, because the energy harvesting is directly correlated to the hydrodynamic performances of the floaters.

IV. Conclusions

This work describes the experimental test setup for the investigation on the hydrodynamic behavior of five floaters moored with a slack mooring system. All the scaling procedures and technology solutions are presented for both the floater and mooring system.

The adoption of the artificial seabed has proved to be a cheap and easy to implement solution to guarantee the desired seabed distance and it can be improved in prevision of other experimental tests. The instrumentation setup preparation for the array tests was complex and challenging. The calibration of the camera acquisition system was not trivial due to the presence of a high number of wave probes close to the calibrated area that that caused unforeseen shadow zones.

In this paper, the first results of this experimental campaign are presented. The free decay analysis of the pitch DoF is done in order to identify the pitch natural period and the linear and quadratic damping terms.

A regular wave analysis is carried out for two different wave steepness 1:50 and 1:35 and two different array configuration are compared with the single device configuration. The dimensionless pitch RAO is taken as performance index to compare the different array configuration.

The 3x1 array configuration shows a similar behavior compared to the single device case for a wave direction of 0 deg. Instead, in the case of the 3x2 array configuration the interaction between the floaters was relevant close to the pitch natural period. Therefore, the analysis can be only qualitative because no stationary condition were reached for these wave tests. The floaters 1, 2, 3, which are positioned upstream present a pitch RAO similar to the single device case and therefore the performance as well are similar. On the other hand, the floaters *4*, *5* are downstream, and they present a strong reduction of performances around the pitch resonance condition, because they are shadowed by the upstream floaters. Therefore, the performances of a WEC array is strongly affected by the chosen layout and WECs positioned downstream are affected negatively by the presence of upstream WECs.

Acknowledgment

The research leading to these results has received funding from the European Union Horizon 2020 Framework Programme (H2020) under grant agreement no 731084.

REFERENCES

[1] B. Drew, A. Plummer, M.N. Sahinkaya, "A review of wave energy converter technology," *Proceedings of the Institution of Mechanical Engineers, Part A: Journal of Power and Energy*, 223 vol. 8, pp. 887-902, 2009.

[2] S. Lindroth, M. Leijon, "Offshore wave power measurements – A review," *Renewable and Sustainable Energy Reviews*, vol. 15, pp. 4274-4285, 2010.

[3] S. De Chowdhury, J. R. Nader, A. Madrigal Sanchez, A. Fleming et al., "A review of hydrodynamic investigations into arrays of ocean wave energy converters," 2015. retrieved February 2, 2016, from,http://arxiv.org/ftp/arxiv/papers/1508/1508.00866.pdf

[4] J. Falnes, "Radiation impedance matrix and optimum power absorption for interacting oscillators in surface waves," *Applied ocean research*, vol. 2, pp. 75–80, 1980.

[5] G.P. Thomas, D. Evans, "Arrays of three-dimensional wave energy absorbers," *Journal of Fluid Mechanics*, vol. 108, pp. 67-88, July 1981.

[6] S.A. Sirigu, G. Vissio, G. Bracco, P. Dafnakis, et al. , "A performance assessment methodology for floating pitching WEC arrays," *Proceedings of the 12th European Wave and Tidal Energy Conference*, Cork, Ireland, 2017

[7] M. Folley, *Numerical Modelling of Wave Energy Converters*, 1st ed., Elsevier Science Publishing Co Inc, 2016

[8] L. Bergdahl and I. Rask, "Dynamic vs. Quasi-Static Design of Catenary Mooring System," *Proceedings of the 19th Offshore Technology Conference*, Houston, Texas, vol. 3, pp. 397-404, 1998.

[9] L. Bergdahl, J. Palm, C. Eskilsson and J. Lindahl, "Dynamically Scaled Model Experiment of a Mooring Cable", Journal of Marine Science and Engineering, vol. 4(1), March 2016.

[10] H.A. Wolgamot and C.J. Fitzgerald, "Nonlinear hydrodynamic and real fluid effects on wave energy converters," *Journal of Power and Energy*, vol. 229, pp. 772-794, 2015.

[11] E.B. Agamloh, A.K. Wallace, A. von Jouanne, "Application of fluid-structure interaction simulation of an ocean wave energy extraction device," *Renewable Energy*, vol. 33, pp. 748-757, 2008.

[12] B. Devolder, V. Stratigaki, P. Troch, P. Rauwoens, "CFD simulations of floating point absorber wave energy converter arrays subjected to regular waves," *energies*, vol. 11(3), pp. 1-23, 2018.

[13] V. Stratigaki, P. Troch, T. Stallard, D. Forehand et al., "Wave Basin Experiments with Large Wave Energy Converter Arrays to Study Interactions between the Converters and Effects on Other Users in the Sea and the Coastal Area," *energies*, vol. 7, pp. 701-734, 2014.

[14] V. Krivtsov and B. Linfoot, "Basin Testing of Wave Energy Converters in Trondheim: Investigation of Mooring Loads and Implications for Wider Research," *Journal of Marine Science and Engineering*, vol. 2, pp. 326-335, 2014.

[15] P.M. Ruiz, F.Ferri, J.P. Kofoed, "Experimental Validation of a Wave Energy Converter Array Hydrodynamics Tool," *Sustainability*, vol. 9(1), 115, 2017.

[16] L. O'Boyle, B. Elsäßer and T. Whittaker, "Experimental Measurement of Wave Field Variations around Wave Energy Converter Arrays," *sustanaibility*, vol. 9(1), pp. 1-16, January 2017.

[17] G. Bracco, E. Giorcelli, G. Giorgi, G. Mattiazzo et al., "Performance assessment of the full scale ISWEC system," *Proceedings of the IEEE International Conference on Industrial Technology*, art no. 7125466, pp. 2499-2505, 2015.

[18] A. Cagninei, M. Raffero, G. Bracco, E. Giorcelli et al., "Productivity analysis of the full scale inertial sea wave energy converter prototype: A test case in Pantelleria Island," *Journal of Renewable and Sustainable Energy*, vol. 7 (6), 2015.

[19] S. A. Sirigu, G. Vissio, G. Bracco, E. Giorcelli, et al., "ISWEC design tool," *International Journal of Marine Energy*, vol. 15, pp. 201-213, September 2016.

[20] E. Begovic, A.H. Day, A. Incecik, "experimental study of hull girder loads on an intact and damaged naval ship," *Ocean Engineering*, vol. 133, pp. 47-65, 2016.

[21] S.K. Chakrabarti, *Offshore structure modelling*, Advanced Series in Ocean Engineering, Worlds Scientific Publishing Co., vol. 9, February 1994

[22] G. Bulian, A. Francescutto, F. Fucile, "Determination of Relevant Parameters for the Alternative Assessment of Intact Stability Weather Criterion On Experimental Basis," On Experimental Basis, Project HYD-III-CEH-5, Rev.1.0-Final-22. Available at www.shipstab.org

[23] ITTC – Recommended Procedures and Guidelines, 2011. Numerical Estimation of Roll Damping. 7.5-02-07-04.5.